

Nonequilibrium noise as a probe of pair-tunneling transport in the BCS–BEC Crossover

Hiroyuki Tajima,^{1,*} Daigo Oue,^{2,3} Mamoru Matsuo,^{3,4,5,6} and Takeo Kato⁷

¹*Department of Physics, Graduate School of Science,
The University of Tokyo, Tokyo, 113-0033, Japan*

²*The Blackett Laboratory, Department of Physics, Imperial College London,
Prince Consort Road, Kensington, London SW7 2AZ, United Kingdom*

³*Kavli Institute for Theoretical Sciences, University of Chinese Academy of Sciences, Beijing, 100190, China.*

⁴*CAS Center for Excellence in Topological Quantum Computation,
University of Chinese Academy of Sciences, Beijing 100190, China*

⁵*Advanced Science Research Center, Japan Atomic Energy Agency, Tokai, 319-1195, Japan*

⁶*RIKEN Center for Emergent Matter Science (CEMS), Wako, Saitama 351-0198, Japan*

⁷*The Institute for Solid State Physics, The University of Tokyo, Kashiwa 277-8581, Japan*
(Dated: March 14, 2023)

The detection of elementary carriers in transport phenomena is one of the most important keys to understand non-trivial properties of strongly-correlated quantum matter. Here we propose a method to identify the tunneling current carrier in strongly interacting fermions from nonequilibrium noise in the Bardeen-Cooper-Schrieffer to Bose–Einstein condensate crossover. The noise-to-current ratio, the Fano factor, can be a crucial probe for the current carrier. Bringing strongly-correlated fermions into contact with a dilute reservoir produces a tunneling current in between. The associated Fano factor increases from one to two as the interaction becomes stronger, reflecting the fact that the dominant conduction channel changes from the quasiparticle tunneling to the pair tunneling.

Transport phenomena have contributed to the development of the fundamental physics in previous centuries. Various unconventional phenomena such as superfluidity and superconductivity were observed using transport measurements. However, clarifying the microscopic mechanism of the transport phenomena in strongly-correlated systems remains challenging because of their complexities such as strong interactions, lattice geometries, as well as multiple degrees of freedom.

Recently, an ultracold atomic system has been regarded as a quantum simulator for strongly-correlated many-body systems such as unconventional superconductors and nuclear systems, owing to its controllability of physical parameters (e.g., interparticle interactions and lattice structures) and its cleanliness [1, 2]. In particular, state-of-the-art experiments for tunneling current have been conducted in strongly interacting Fermi gases [3–8]. Moreover, thermoelectric transport has been demonstrated experimentally in an ultracold Fermi gas [9]. A quantum point contact has also been implemented for atomic superfluid junctions [10]. These experiments motivate us to study tunneling transport associated with the Josephson effect and Cooper-pair tunneling in the superfluid phase of the Bardeen-Cooper-Schrieffer (BCS) to Bose–Einstein-condensate (BEC) crossover [11–19]. Such a direction are recently referred to as *atomtronics* [20].

One crucial problem is to understand how strong correlations affect the conduction mechanism, which is necessary for future development of quantum-transport technology. Recently, several theoretical efforts have been

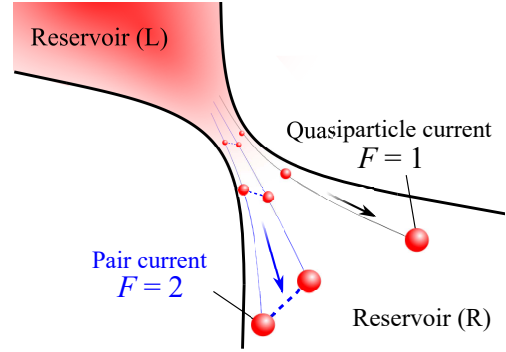


FIG. 1. Strongly interacting quantum gases (reservoirs L and R) with a large chemical-potential bias in between. The Fano factor F can be regarded as an indicator of the current carrier, i.e., quasiparticle current ($F = 1$) and the pair current ($F = 2$).

paid to understand an anomalous tunneling current induced by pairing fluctuations in the normal phase [21–24], as observed in experiments [3–8]. It is anticipated that such anomalous pair-tunneling currents can be induced by the nonlinear tunneling processes [21], tunneling of a closed-channel molecule [22], and the proximity effect associated with two-body interactions [25]. However, regardless of these different origins, the existence of the pair-tunneling current itself is still an important pending problem because it is difficult to distinguish quasiparticle- and pair-tunneling currents experimentally. In this sense, it is worth exploring clear evidence for anomalous pair currents in a strongly interacting Fermi gas.

For this purpose, measuring the Fano factor is promis-

* hiroyuki.tajima@phys.s.u-tokyo.ac.jp

ing, which is defined by a current and the associated nonequilibrium noise [26, 27]. The Fano factor in the large-biased setup reflects the effective charge per elementary transport process regardless of system's detail. The most fascinating example is the detection of fractional charges in fractional quantum Hall systems [28, 29]. The Fano factor has been used to determine the effective charge (or spin) in various physical systems such as superconductors [30, 31], Kondo quantum dots [32, 33], and magnetic junctions [34–37]. Once the Fano factor is measured in strongly interacting Fermi gases, the existence of the pair-tunneling current will be revealed in an unbiased way.

In this study, we show that the Fano factor F can be used as a probe for the current carrier in the BCS–BEC crossover. Figure 1 shows a schematic setup of the large-biased system. Using the many-body T -matrix approach (TMA) [38, 39], we numerically calculate the current and nonequilibrium noise within the Schwinger–Keldysh approach in the two-terminal tunneling junction under a large bias. We reveal how the Fano factor F changes in a strongly-interacting regime, thereby reflecting the change of the dominant carrier. In particular, the change of F is a crucial evidence for the pair-tunneling current. Our result can be tested by cold-atom experiments for which the noise measurement has been theoretically proposed [40]. Moreover, the Fano factor provides direct information of pair-fluctuation effects rather than other measurements such as spin susceptibility and photoemission spectra previously studied in this field [41]. The current-noise measurement can also be used to identify the carriers of the BCS–BEC crossover in condensed-matter systems such as FeSe semimetal [42–45], lithium-intercalated layered nitrides [46, 47], magic-angle twisted trilayer graphene [48], and organic superconductor [49]. Moreover, the noise measurement has recently been conducted in a copper oxide heterostructure [50, 51] and disordered superconductor [52].

In the following, we take $\hbar = k_B = 1$ and consider a unit volume.

TUNNELING CURRENT AND NOISE

We consider the Hamiltonian $H = H_L + H_R + H_{1T} + H_{2T}$. The reservoir Hamiltonian $H_{j=L,R}$ is given by

$$H_j = \sum_{\mathbf{p},\sigma} \xi_{\mathbf{p},j} c_{\mathbf{p},\sigma,j}^\dagger c_{\mathbf{p},\sigma,j} + g \sum_{\mathbf{q}} P_{\mathbf{q},j}^\dagger P_{\mathbf{q},j}, \quad (1)$$

where $\xi_{\mathbf{p},j} = p^2/(2m) - \mu_j$ denotes the kinetic energy measured from the chemical potential μ_j and $c_{\mathbf{p},\sigma,j}$ denotes the annihilation operator of a Fermi atom with momentum \mathbf{p} and the pseudospin $\sigma = \uparrow, \downarrow$. The second term in Eq. (1) denotes the attractive interaction with a contact-type coupling g , where $P_{\mathbf{q},j} = \sum_{\mathbf{p}} c_{-\mathbf{p}+\mathbf{q}/2,\downarrow,j} c_{\mathbf{p}+\mathbf{q}/2,\uparrow,j}$ is the pair-annihilation operator and g is related to the scattering length a as $\frac{m}{4\pi a} = \frac{1}{g} + \sum_{\mathbf{p}} \frac{m}{p^2}$ [39].

The one-body tunneling Hamiltonian,

$$H_{1T} = \sum_{\mathbf{p},\mathbf{k},\sigma} \left[t_{\mathbf{p},\mathbf{k}} c_{\mathbf{p},\sigma,L}^\dagger c_{\mathbf{k},\sigma,R} + \text{h.c.} \right], \quad (2)$$

is associated with the one-body potential barrier, where $t_{\mathbf{p},\mathbf{k}}$ denotes its coupling strength. The two-body tunneling Hamiltonian reads

$$H_{2T} = \sum_{\mathbf{q},\mathbf{q}'} \left[w_{\mathbf{q},\mathbf{q}'} P_{\mathbf{q},L}^\dagger P_{\mathbf{q}',R} + \text{h.c.} \right], \quad (3)$$

where $w_{\mathbf{q},\mathbf{q}'}$ is the two-body coupling strength, induced by the local interaction term in Eq. (1) combined with the one-body potential barrier [25]. Such two-body tunneling processes can also be obtained within the multiple one-body tunneling processes in the nonlinear regime [17, 21, 24, 53]. We note that regardless of their origins, these two-body tunnelings induce the pair-tunneling current. Similar tunneling effects have also been examined in one-dimensional few-body systems [54, 55]. Here, we do not go into details on the origin of the one- and two-body tunneling, but rather investigate their possible consequence in observable quantities. However, we emphasize that the two-body tunneling term is necessary to describe the molecule tunneling in the deep BEC side (and therefore the entire crossover), where the pair-tunneling induced by the higher-order one-body tunneling process is suppressed due to the reduced dissociation of molecules with the large binding energy [24]. In Fig. S1 of the supplement [56], we estimate the tunneling couplings in the case of delta-function-like potential barrier [19, 57] based on Ref. [25].

Using the Schwinger–Keldysh approach, we evaluate the expectation values of the current operator $\hat{I} = i[\hat{N}_L, H]$ ($\hat{N}_j = \sum_{\mathbf{p},\sigma} c_{\mathbf{p},\sigma,j}^\dagger c_{\mathbf{p},\sigma,j}$ denotes the density operator in the j -reservoir) in the steady state at the lowest-order tunneling couplings by a sum of the one- and two-body contributions as $I = I_{\text{qp}} + I_{\text{pair}}$, where each component reads [25, 56]

$$\begin{aligned} I_{\text{qp}} &= \int_{-\infty}^{\infty} \frac{d\omega}{2\pi} \sum_{\mathbf{p},\mathbf{k},\sigma} |t_{\mathbf{k},\mathbf{p}}|^2 \mathcal{A}_{\mathbf{k},L}(\omega) \mathcal{A}_{\mathbf{p},R}(\omega) \\ &\quad \times [f_L(\omega) - f_R(\omega)], \\ I_{\text{pair}} &= 2 \int_{-\infty}^{\infty} \frac{d\omega}{2\pi} \sum_{\mathbf{q},\mathbf{q}'} |w_{\mathbf{q},\mathbf{q}'}|^2 \mathcal{B}_{\mathbf{q},L}(\omega) \mathcal{B}_{\mathbf{q}',R}(\omega) \\ &\quad \times [b_L(\omega) - b_R(\omega)]. \end{aligned} \quad (4)$$

In Eq. (4), $\mathcal{A}_{\mathbf{k},j}(\omega)$ and $\mathcal{B}_{\mathbf{q},j}(\omega)$ denote one- and two-particle spectral functions, respectively, $f_j(\omega)$ and $b_j(\omega)$ denotes the Fermi and Bose distribution functions, and $\mu_{b,j} = 2\mu_j$ denotes the bosonic-pair chemical potential in the j -reservoir. For the detection of the pair-tunneling current, it is crucial to consider the small tunneling coupling regime where the nonequilibrium noise reflects an effective particle number in tunneling process. [58]

We define the current noise as $\bar{\mathcal{S}}(t_1, t_2) = \frac{1}{2} \langle \hat{I}(t_1) \hat{I}(t_2) + \hat{I}(t_2) \hat{I}(t_1) \rangle$ [59–62] [see also, e.g.,

Ref. [36]]. For the steady-state transport with the time-translational symmetry, we assume that the noise depends on $t_1 - t_2$ as $\bar{S}(t_1, t_2) \equiv \bar{S}(t_1 - t_2)$ (being independent of $\frac{t_1+t_2}{2}$). Its Fourier component reads

$$\bar{S}(\omega) = \frac{1}{\tau} \int_0^\tau dt_1 \int_0^\tau dt_2 e^{i\omega(t_1-t_2)} \bar{S}(t_1 - t_2), \quad (5)$$

where τ is the typical time scale for the noise measurement. Taking $t = t_1 - t_2$ and $\bar{S}(t) = \frac{1}{2}(\hat{I}(t)\hat{I}(0) + \hat{I}(0)\hat{I}(t))$, we obtain the zero-frequency limit of the noise power $S \equiv \bar{S}(\omega \rightarrow \eta)$ (η is an infinitesimally small number) as

$$S = \frac{1}{2} \int_{-\infty}^{\infty} dt \left(\langle \hat{I}(t)\hat{I}(0) \rangle + \langle \hat{I}(0)\hat{I}(t) \rangle \right), \quad (6)$$

where we considered the limit of $\tau \rightarrow \infty$. In this regard, we briefly note that τ should be sufficiently longer than the transport timescale τ_0 , where in the recent experiment $\tau_0 = O(10^{-1})$ s is found [9]. Similar to the calculation above, we can evaluate the current noise [56] as the sum of the two contributions: $S = S_{\text{qp}} + S_{\text{pair}}$, where

$$\begin{aligned} S_{\text{qp}} &= \int_{-\infty}^{\infty} \frac{d\omega}{2\pi} \sum_{\mathbf{p}, \mathbf{k}, \sigma} |t_{\mathbf{k}, \mathbf{p}}|^2 \mathcal{A}_{\mathbf{k}, \text{L}}(\omega) \mathcal{A}_{\mathbf{p}, \text{R}}(\omega) \\ &\quad \times [f_{\text{L}}(\omega)\{1 - f_{\text{R}}(\omega)\} + \{1 - f_{\text{L}}(\omega)\}f_{\text{R}}(\omega)], \\ S_{\text{pair}} &= 4 \int_{-\infty}^{\infty} \frac{d\omega}{2\pi} \sum_{\mathbf{q}, \mathbf{q}'} |w_{\mathbf{q}, \mathbf{q}'}|^2 \mathcal{B}_{\mathbf{q}, \text{L}}(\omega) \mathcal{B}_{\mathbf{q}', \text{R}}(\omega) \\ &\quad \times [b_{\text{L}}(\omega)\{1 + b_{\text{R}}(\omega)\} + b_{\text{R}}(\omega)\{1 + b_{\text{L}}(\omega)\}]. \end{aligned} \quad (7)$$

The bias between the reservoirs is included in the distribution function and therefore (7) is valid for the case with the temperature bias [63]. In the large chemical potential bias limit ($\Delta\mu \equiv \mu_{\text{L}} - \mu_{\text{R}} \rightarrow \infty$), we can prove $S_{\text{qp}}/I_{\text{qp}} = 1$ and $S_{\text{pair}}/I_{\text{pair}} = 2$ without any further approximations [56]. This motivates us to consider the Fano factor,

$$F = \frac{S}{I} = \frac{S_{\text{qp}} + S_{\text{pair}}}{I_{\text{qp}} + I_{\text{pair}}}. \quad (8)$$

The Fano factor F changes from 1 to 2, according to whether the quasiparticle or pair tunneling is dominant and hence, it is a useful probe for the current carrier. In particular, the Fano factor F becomes 1 and 2 in the BCS limit ($a^{-1} \rightarrow -\infty$) and BEC limit ($a^{-1} \rightarrow \infty$), respectively. Importantly, the deviation of F from 1 indicates a clear evidence of the pair-tunneling process yet to be not well understood in cold atomic systems [25]. Therefore, the observation of F can be a crucial key for understanding transport phenomena in strongly interacting systems.

In this study, we consider the large bias regime (see Fig. 1) characterized by $\mu_{\text{L}} - \mu_{\text{R}} \rightarrow \infty$ [56, 64] and the momentum-conserved tunneling processes as $t_{\mathbf{p}, \mathbf{k}} = T_1 \delta_{\mathbf{p}, \mathbf{k}}$ and $w_{\mathbf{q}, \mathbf{q}'} = T_2 \delta_{\mathbf{q}, \mathbf{q}'}$, for simplicity. To see the

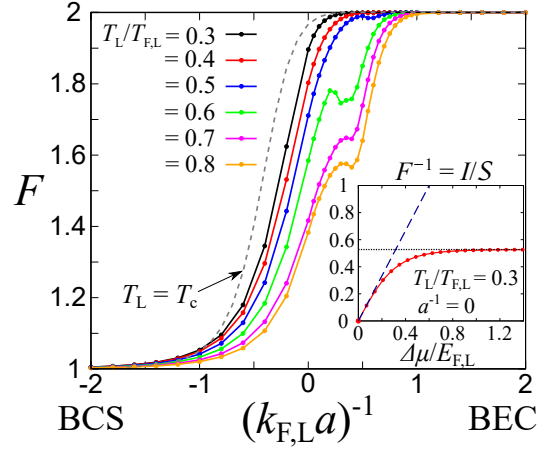


FIG. 2. Fano factor F , associated with tunneling transport between two reservoirs, throughout the BCS-BEC crossover for various temperatures T_{L} in the reservoir L. The reservoir R is almost vacuum. The ratio between tunneling couplings is given as $T_{2,\text{ren.}}/T_1 = 1$. For comparison, we plot the result at $T_{\text{L}} = T_{\text{c}}$ (dashed curve). Note that T_{c} changes in the range of $0.02T_{\text{F,L}} \lesssim T_{\text{c}} \lesssim 0.24T_{\text{F,L}}$ depending on $(k_{\text{F,L}}a)^{-1}$. The inset shows the bias ($\Delta\mu$) dependence of F^{-1} at $T_{\text{L}}/T_{\text{F,L}} = 0.3$ and $a^{-1} = 0$. The dashed and dotted lines represent the Onsager's relation $F^{-1}(\Delta\mu \rightarrow 0) = \frac{\Delta\mu}{2T}$ [56] and the large bias limit, respectively.

qualitative behavior of F , we use the spectral functions $\mathcal{A}_{\mathbf{k}, \text{j}}(\omega) = -2 \text{Im} G_{\mathbf{k}, \text{j}}(i\omega_n \rightarrow \omega - \mu_{\text{j}} + i\eta)$ and $\mathcal{B}_{\mathbf{q}, \text{j}}(\omega) = -2 \text{Im} \mathcal{G}_{\mathbf{q}, \text{j}}(i\nu_\ell \rightarrow \omega - \mu_{\text{b,j}} + i\eta)$ with an infinitesimal small number η , where thermal single- and two-particle propagators $G_{\mathbf{k}, \text{j}}(i\omega_n)$ and $\mathcal{G}_{\mathbf{q}, \text{j}}(i\nu_\ell)$ with fermion and boson Matsubara frequencies $i\omega_n$ and $i\nu_\ell$ are evaluated within the many-body TMA [65, 66] (see also Supplemental Material [56]). We employ $\eta = 10^{-2}E_{\text{F,L}}$ in the numerical calculation to avoid the divergent behavior of the current associated with the momentum-conserved tunneling in the weak- and strong-coupling limits, where $E_{\text{F,L}} = (3\pi^2 N_{\text{L}})^{2/3}/(2m)$ denotes the Fermi energy of the L reservoir with the number density N_{L} . However, our result can be qualitatively unchanged by this treatment because the distribution functions play a key role in determining F rather than the detailed structures of tunneling junctions. Moreover, T_2 must be normalized to suppress the ultraviolet divergence in $B_{\mathbf{q}, \text{j}}(\omega)$. For this purpose, we introduce the renormalized two-body tunneling coupling $T_{2,\text{ren.}} = \frac{\Lambda^2 k_{\text{F,L}}}{3\sqrt{2}\pi^2} T_2$ where $k_{\text{F,L}} = \sqrt{2mE_{\text{F,L}}}$ denotes the Fermi momentum. Such a divergence can also be avoided by introducing the form factor for the relative momentum \mathbf{p} in $P_{\mathbf{q}, \text{j}}$ [67]. In this work, we take $\Lambda = 100k_{\text{F,L}}$ [39] in the practical calculation. This value is associated with the effective range r_{eff} as $r_{\text{eff}} = \frac{4}{\pi\Lambda}$ [39].

FANO FACTOR THROUGHOUT THE BCS-BEC CROSSOVER

Fig. 2 shows the Fano factor F as a function of the dimensionless interaction parameter $(k_{F,L}a)^{-1}$ in the entire BCS-BEC crossover regime above the superfluid critical temperature T_c . We considered $\mathcal{T}_{2,\text{ren.}}/\mathcal{T}_1 = 1$, and the reservoir R was regarded as almost vacuum ($\mu_L - \mu_R \rightarrow \infty$) [56]. As we showed in the inset of Fig. 2, the large-bias assumption can be justified when $\Delta\mu$ is larger than a typical many-body scale in the reservoir (i.e., $E_{F,L}$). One can clearly see that F evolves from 1 to 2 with increasing the interaction strength in Fig. 2, indicating that the current carrier gradually changes from quasiparticles ($F = 1$) to pairs ($F = 2$). Such a behavior is universal in the sense that these asymptotic values do not depend on any details on the model parameters and structures of tunneling junctions. More explicitly, at the large bias limit, one can obtain [56]

$$F(\Delta\mu \rightarrow \infty) \rightarrow \frac{I_{\text{qp}} + 2I_{\text{pair}}}{I_{\text{qp}} + I_{\text{pair}}}, \quad (9)$$

where I_{qp} and I_{pair} denote the contributions of the quasiparticle and pair tunnelings, respectively. The Fano factor F approaches 1 and 2 in the quasiparticle-dominant ($I_{\text{qp}} \gg I_{\text{pair}}$) and pair-dominant regimes ($I_{\text{pair}} \gg I_{\text{qp}}$), respectively. Although the interaction dependence of the Fano factor F is deeply related to properties of the tunneling junctions and spectral functions of the carriers, one can find from Eq. (9) that $F \rightarrow 1$ ($F \rightarrow 2$) in the limit of $a^{-1} \rightarrow -\infty$ ($a^{-1} \rightarrow \infty$) regardless of the detailed properties of the system. Moreover, $F = 2$ can be realized even above T_c because of strong interactions leading to the formation of preformed Cooper pairs in the BCS-BEC crossover. With increasing the temperature, F tends to be suppressed because thermal effects assist the dissociation of pairs. Nevertheless, even at finite temperature, F approaches 2 with increasing the interaction because bound molecules are dominant in the deep BEC regime [68] where $T_L \lesssim E_b$ [$E_b = 1/(ma^2)$ is the two-body binding energy].

To see the detailed behavior of the Fano factor F , we plot I_{qp} and I_{pair} throughout the BCS-BEC crossover at different temperatures in Fig. 3. From the inset of Fig. 3, the quasiparticle current I_{qp} is exponentially suppressed with increasing the attractive interaction. This suppression (in particular, the rapid drop of I_{qp} at $(k_{F,L}a)^{-1} \gtrsim -0.5$) is induced by the pairing fluctuation effect [39], i.e., the reduction of $\mathcal{A}_{\mathbf{k},L}(\omega)$ near $|\mathbf{k}| = k_{F,L}$ and $\omega = E_{F,L}$ ($\simeq \mu_L$) by the particle-hole coupling. We note that this fluctuation effects result in the pseudogap in the density of state near T_c [41]. Finally, I_{qp} approaches zero in the BEC limit ($(k_{F,L}a)^{-1} \rightarrow \infty$) because of the formation of molecules with large binding energies. These results are qualitatively consistent with previous work [21, 24]. On the other hand, I_{pair} drastically increases with increasing the interaction strength $(k_{F,L}a)^{-1}$ as shown in Fig. 3. At the BCS side ($(k_{F,L}a)^{-1} < 0$)

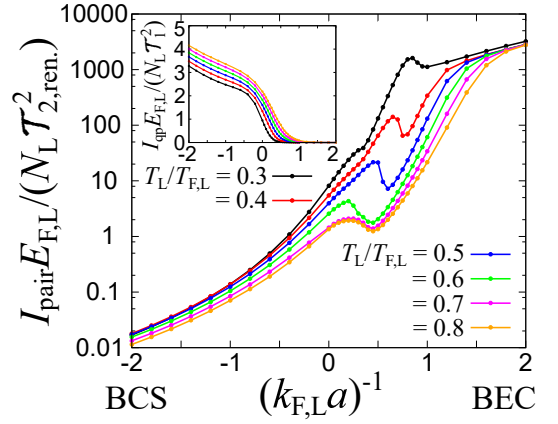


FIG. 3. Pair-tunneling current I_{pair} in the normal phase throughout the BCS-BEC crossover at different temperatures. The inset shows the quasiparticle current I_{qp} with the same horizontal axis $(k_{F,L}a)^{-1}$.

where the attraction is not strong to form a two-body bound state in vacuum, the contribution of I_{pair} can be regarded as the tunneling of the preformed Cooper pairs into the two-body continuum in the reservoir R. In the strong-coupling BEC regime ($(k_{F,L}a)^{-1} > 1$ and $T_L/E_b \lesssim 1$), I_{pair} describes the tunneling transport of bound molecules across two reservoirs, because the two-body bound state exists in the reservoir R with the same coupling g . Such a tunneling current associated with weakly-interacting molecular bosons becomes large due to their long lifetime and the Bose enhancement of low-energy distributions.

One can also see a dip-hump structure of I_{pair} in the intermediate regime. Here, μ_L is close to zero and changes its sign, indicating that the dominant contribution changes from the preformed-pair transfer to the molecule-to-molecule transport across the junction. From the unitary limit ($(k_{F,L}a)^{-1} = 0$), the preformed-pair transfer increases due to the overlap with the bound-state spectra in $B_{\mathbf{q},R}(\omega)$ and eventually decreases because of the decrease in μ_L . With increasing the interaction further, the inter-reservoir molecule-to-molecule transition emerges where the bound-state spectra in two reservoirs get close to each other in the energy axis ω [69]. Although these structures reflect the physical properties of the system, they also depend on the detailed setup of the tunneling junctions (e.g., the ratio between the tunneling couplings $\mathcal{T}_{2,\text{ren.}}/\mathcal{T}_1$) [56].

Figure 4 shows the temperature dependence of the Fano factor F in the unitary limit ($(k_{F,L}a)^{-1} = 0$). Because $\mathcal{B}_{\mathbf{q},R}(\omega)$ does not involve a bound molecule pole, the transfer of the preformed Cooper pairs in the reservoir L to the two-body continuum in the reservoir R can be anticipated in the unitary limit. One can see the enhancement of the Fano factor F at the low-temperature regime. In particular, the curvature of the Fano factor F is modified at $T_L/T_c \simeq 2.8$, where the sign of μ_L changes from negative to positive one as the tempera-

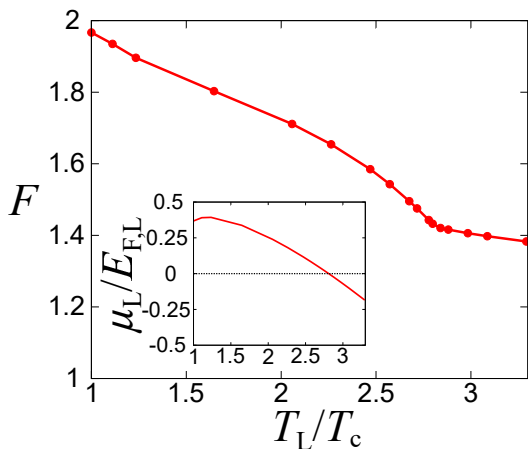


FIG. 4. Temperature dependence of the Fano factor F in the unitary limit [$1/(k_{F,L}a) = 0$] with $\mathcal{T}_{2,\text{ren.}}/\mathcal{T}_1 = 1$. The horizontal axis is taken as T_L/T_c , where T_c is the superfluid critical temperature. The inset shows the chemical potential μ_L as a function of T_L/T_c for a given Fermi energy $E_{F,L}$.

ture decreases (see the inset of Fig. 4). Although the Fano factor depends on $\mathcal{T}_{2,\text{ren.}}/\mathcal{T}_1$ as shown in Fig. S2 of the supplement [56], the qualitative behavior, i.e., suppression of the pair-tunneling current due to increase of the temperature is unchanged regardless of the value of $\mathcal{T}_{2,\text{ren.}}/\mathcal{T}_1$. For estimating the value of $\mathcal{T}_{2,\text{ren.}}/\mathcal{T}_1$ (which depends on the potential barrier and the interaction strength) in each experimental setup, see Ref. [25]. In the supplement [56], we show that $\mathcal{T}_{2,\text{ren.}}/\mathcal{T}_1$ can be tuned and it is possible to realize $\mathcal{T}_{2,\text{ren.}}/\mathcal{T}_1 \simeq 1$ by adjusting the strength of the potential barrier as $\mathcal{T}_{2,\text{ren.}}/\mathcal{T}_1 \propto \left(1 + \frac{V_0}{E_{F,L}}\right)^{-1} \left[1 + \left(\frac{V_0}{E_{F,L}}\right)^2 (k_{F,L}\ell)^2\right]^{-1/2}$ for the potential barrier given by $V = V_0\delta(x/\ell)$ perpendicular to the x axis (V_0 and ℓ are the strength and the characteristic length scale of the barrier). At a positive μ_L , the pole of the preformed Cooper pairs gradually appears in $\mathcal{B}_{q,L}(\omega)$. Thus, the behavior of the Fano factor F can be regarded as a signature of the preformed Cooper pairs. Because the preformed Cooper pairs play an important role in the pseudogap physics of ultracold Fermi gases [41], the Fano factor contributes to the further understanding of pairing pseudogaps in the BCS-BEC crossover regime. Incidentally, because TMA does not capture the self-energy

shift in $\Pi_{q,L}(\omega)$, the curvature change of the Fano factor F may differ from the temperature where $\mu_L = 0$ in actual experiments and in more sophisticated theoretical approaches [38, 39]. To evaluate the spectral functions, the analytic continuation should be carefully performed in Monte Carlo simulations [70]. We note that because TMA reproduces the second-order virial expansion [71], our result in the relatively high-temperature regime can give an accurate estimate of F for given tunnel couplings.

SUMMARY

In this study, we showed that the Fano factor (i.e., the noise-to-current ratio $F = \mathcal{S}/I$) can be a useful probe for current carriers in the BCS-BEC crossover at large-biased tunneling junctions. Using the many-body TMA, we demonstrated that the Fano factor F gradually changes from one to two as the interaction strength increases in the normal phase, indicating that the dominant current carrier changes from the quasiparticle ($F = 1$) to the pair ($F = 2$) along the BCS-BEC crossover. Our prediction can be tested by experiments and uncover nonequilibrium strong-coupling physics via transport measurements. While we have focused on the large bias limit, such a situation can be achieved when the bias is larger than the many-body energy scale (i.e., Fermi energy of the dense reservoir). Furthermore, our result indicates that the noise measurement is useful for the study of the BCS-BEC crossover and pair-fluctuation effects in unconventional superconductors.

ACKNOWLEDGMENTS

This work is supported in part by Grants-in-Aid for Scientific Research from JSPS (Grants Nos. JP18H05406, JP20K03831, 22K13981). D.O. is supported by the President's PhD Scholarships at Imperial College London, by JSPS Overseas Research Fellowship, by the Institution of Engineering and Technology (IET), and by Fundação para a Ciência e a Tecnologia and Instituto de Telecomunicações under project UIDB/50008/2020. MM is partially supported by the Priority Program of the Chinese Academy of Sciences, Grant No. XDB28000000. This manuscript was posted on a preprint: <https://doi.org/10.48550/arXiv.2202.03873>

-
- [1] I. Bloch, J. Dalibard, and W. Zwerger, Many-body physics with ultracold gases, *Rev. Mod. Phys.* **80**, 885 (2008).
 - [2] C. Chin, R. Grimm, P. Julienne, and E. Tiesinga, Feshbach resonances in ultracold gases, *Rev. Mod. Phys.* **82**, 1225 (2010).
 - [3] S. Krinner, M. Lebrat, D. Husmann, C. Grenier, J.-P. Brantut, and T. Esslinger, Mapping out spin and particle conductances in a quantum point contact,

Proceedings of the National Academy of Sciences **113**, 8144 (2016), <https://www.pnas.org/content/113/29/8144.full.pdf>.

- [4] S. Häusler, S. Nakajima, M. Lebrat, D. Husmann, S. Krinner, T. Esslinger, and J.-P. Brantut, Scanning gate microscope for cold atomic gases, *Phys. Rev. Lett.* **119**, 030403 (2017).
- [5] W. Kwon, G. Del Pace, R. Panza, M. Inguscio, W. Zwerger, M. Zaccanti, F. Scazza, and G. Roati, Strongly correlated superfluid order parameters from dc Joseph-

- son supercurrents, *Science* **369**, 84 (2020).
- [6] N. Luick, L. Sobirey, M. Bohlen, V. P. Singh, L. Mathey, T. Lompe, and H. Moritz, An ideal josephson junction in an ultracold two-dimensional fermi gas, *Science* **369**, 89 (2020).
 - [7] G. Del Pace, W. J. Kwon, M. Zaccanti, G. Roati, and F. Scazza, Tunneling transport of unitary fermions across the superfluid transition, *Phys. Rev. Lett.* **126**, 055301 (2021).
 - [8] S. Häusler, P. Fabritius, J. Mohan, M. Lebrat, L. Corman, and T. Esslinger, Interaction-assisted reversal of thermopower with ultracold atoms, *Phys. Rev. X* **11**, 021034 (2021).
 - [9] J.-P. Brantut, C. Grenier, J. Meineke, D. Stadler, S. Krinner, C. Kollath, T. Esslinger, and A. Georges, A thermoelectric heat engine with ultracold atoms, *Science* **342**, 713 (2013).
 - [10] D. Husmann, S. Uchino, S. Krinner, M. Lebrat, T. Giamarchi, T. Esslinger, and J.-P. Brantut, Connecting strongly correlated superfluids by a quantum point contact, *Science* **350**, 1498 (2015).
 - [11] L. Salasnich, N. Manini, and F. Toigo, Macroscopic periodic tunneling of fermi atoms in the bcs-bec crossover, *Phys. Rev. A* **77**, 043609 (2008).
 - [12] M. Kanász-Nagy, L. Glazman, T. Esslinger, and E. A. Demler, Anomalous conductances in an ultracold quantum wire, *Phys. Rev. Lett.* **117**, 255302 (2016).
 - [13] J. Yao, B. Liu, M. Sun, and H. Zhai, Controlled transport between fermi superfluids through a quantum point contact, *Phys. Rev. A* **98**, 041601 (2018).
 - [14] F. Damanet, E. Mascarenhas, D. Pekker, and A. J. Daley, Reservoir engineering of cooper-pair-assisted transport with cold atoms, *New Journal of Physics* **21**, 115001 (2019).
 - [15] M. Zaccanti and W. Zwerger, Critical josephson current in bcs-bec-crossover superfluids, *Phys. Rev. A* **100**, 063601 (2019).
 - [16] V. Piselli, S. Simonucci, and G. C. Strinati, Josephson effect at finite temperature along the bcs-bec crossover, *Physical Review B* **102**, 144517 (2020).
 - [17] S. Uchino, Role of nambu-goldstone modes in the fermionic-superfluid point contact, *Phys. Rev. Research* **2**, 023340 (2020).
 - [18] F. Setiawan and J. Hofmann, Analytic approach to transport in josephson junctions beyond the andreev approximation: General theory and applications to the bec-bcs crossover, *arXiv* **:2108.10333** (2021).
 - [19] D. Zhang and A. T. Sommer, Transport of spin and mass at normal-superfluid interfaces in the unitary fermi gas, *Phys. Rev. Research* **4**, 023231 (2022).
 - [20] L. Amico, M. Boshier, G. Birkel, A. Minguzzi, C. Miniatura, L.-C. Kwek, D. Aghamalyan, V. Ahufinger, D. Anderson, N. Andrei, *et al.*, Roadmap on atomtronics: State of the art and perspective, *AVS Quantum Science* **3**, 039201 (2021).
 - [21] S. Uchino and M. Ueda, Anomalous transport in the superfluid fluctuation regime, *Phys. Rev. Lett.* **118**, 105303 (2017).
 - [22] B. Liu, H. Zhai, and S. Zhang, Anomalous conductance of a strongly interacting fermi gas through a quantum point contact, *Phys. Rev. A* **95**, 013623 (2017).
 - [23] Y. Sekino, H. Tajima, and S. Uchino, Mesoscopic spin transport between strongly interacting fermi gases, *Phys. Rev. Research* **2**, 023152 (2020).
 - [24] K. Furutani and Y. Ohashi, Strong-coupling effects on quantum transport in an ultracold fermi gas, *Journal of Low Temperature Physics* **201**, 49 (2020).
 - [25] H. Tajima, D. Oue, and M. Matsuo, Multiparticle tunneling transport at strongly correlated interfaces, *Phys. Rev. A* **106**, 033310 (2022).
 - [26] Y. M. Blanter and M. Büttiker, Shot noise in mesoscopic conductors, *Phys. Rep.* **336**, 1 (2000).
 - [27] T. Martin, Noise in mesoscopic physics, in *nanophysics: Coherence and transport*, les houches session lxxxii (Elsevier, 2005) Chap. 5.
 - [28] R. de Picciotto, M. Reznikov, M. Heiblum, V. Umansky, G. Bunin, and D. Mahalu, Direct observation of a fractional charge, *Nature* **389**, 162 (1997).
 - [29] L. Saminadayar, D. C. Glatthli, Y. Jin, and B. Etienne, Observation of the $e/3$ fractionally charged Laughlin quasiparticle, *Phys. Rev. Lett.* **79**, 2526 (1997).
 - [30] X. Jehl, M. Sanquer, R. Calemczuk, and D. Mailly, Detection of doubled shot noise in short normal-metal/superconductor junctions, *Nature* **405**, 50 (2000).
 - [31] A. A. Kozhevnikov, R. J. Schoelkopf, and D. E. Prober, Observation of photon-assisted noise in a diffusive normal metal-superconductor junction, *Phys. Rev. Lett.* **84**, 3398 (2000).
 - [32] O. Zarchin, M. Zaffalon, M. Heiblum, D. Mahalu, and V. Umansky, Two-electron bunching in transport through a quantum dot induced by kondo correlations, *Phys. Rev. B* **77**, 241303 (2008).
 - [33] M. Ferrier, T. Arakawa, T. Hata, R. Fujiwara, R. Delagrange, R. Weil, R. Deblock, R. Sakano, A. Oguri, and K. Kobayashi, Universality of non-equilibrium fluctuations in strongly correlated quantum liquids, *Nature Physics* **12**, 230 (2016).
 - [34] A. Kamra and W. Belzig, Super-poissonian shot noise of squeezed-magnon mediated spin transport, *Phys. Rev. Lett.* **116**, 146601 (2016).
 - [35] A. Kamra and W. Belzig, Magnon-mediated spin current noise in ferromagnet | nonmagnetic conductor hybrids, *Phys. Rev. B* **94**, 014419 (2016).
 - [36] M. Matsuo, Y. Ohnuma, T. Kato, and S. Maekawa, Spin current noise of the spin seebeck effect and spin pumping, *Phys. Rev. Lett.* **120**, 037201 (2018).
 - [37] J. Aftergood and S. Takei, Noise in tunneling spin current across coupled quantum spin chains, *Phys. Rev. B* **97**, 014427 (2018).
 - [38] G. C. Strinati, P. Pieri, G. Röpke, P. Schuck, and M. Urban, The bcs-bec crossover: From ultra-cold fermi gases to nuclear systems, *Physics Reports* **738**, 1 (2018), the BCS-BEC crossover: From ultra-cold Fermi gases to nuclear systems.
 - [39] Y. Ohashi, H. Tajima, and P. van Wyk, Bcs-bec crossover in cold atomic and in nuclear systems, *Progress in Particle and Nuclear Physics* **111**, 103739 (2020).
 - [40] S. Uchino, M. Ueda, and J.-P. Brantut, Universal noise in continuous transport measurements of interacting fermions, *Phys. Rev. A* **98**, 063619 (2018).
 - [41] E. J. Mueller, Review of pseudogaps in strongly interacting fermi gases, *Reports on Progress in Physics* **80**, 104401 (2017).
 - [42] Y. Lubashevsky, E. Lahoud, K. Chashka, D. Podolsky, and A. Kanigel, Shallow pockets and very strong coupling superconductivity in $\text{FeSe}_{1-x}\text{Te}_x$, *Nature Physics* **8**, 309 (2012).

- [43] S. Kasahara, T. Watashige, T. Hanaguri, Y. Kohsaka, T. Yamashita, Y. Shimoyama, Y. Mizukami, R. Endo, H. Ikeda, K. Aoyama, *et al.*, Field-induced superconducting phase of fese in the bcs-bec cross-over, *Proceedings of the National Academy of Sciences* **111**, 16309 (2014).
- [44] S. Rinott, K. Chashka, A. Ribak, E. D. Rienks, A. Taleb-Ibrahimi, P. Le Fevre, F. Bertran, M. Randeria, and A. Kanigel, Tuning across the bcs-bec crossover in the multiband superconductor fe1+ ysextel- x: An angle-resolved photoemission study, *Science advances* **3**, e1602372 (2017).
- [45] T. Hanaguri, S. Kasahara, J. Böker, I. Eremin, T. Shibauchi, and Y. Matsuda, Quantum vortex core and missing pseudogap in the multiband bcs-bec crossover superconductor fese, *Physical review letters* **122**, 077001 (2019).
- [46] Y. Nakagawa, Y. Saito, T. Nojima, K. Inumaru, S. Yamanaka, Y. Kasahara, and Y. Iwasa, Gate-controlled low carrier density superconductors: Toward the two-dimensional bcs-bec crossover, *Phys. Rev. B* **98**, 064512 (2018).
- [47] Y. Nakagawa, Y. Kasahara, T. Nomoto, R. Arita, T. Nojima, and Y. Iwasa, Gate-controlled bcs-bec crossover in a two-dimensional superconductor, *Science* **372**, 190 (2021).
- [48] J. M. Park, Y. Cao, K. Watanabe, T. Taniguchi, and P. Jarillo-Herrero, Tunable strongly coupled superconductivity in magic-angle twisted trilayer graphene, *Nature* **590**, 249 (2021).
- [49] Y. Suzuki, K. Wakamatsu, J. Ibuka, H. Oike, T. Fujii, K. Miyagawa, H. Taniguchi, and K. Kanoda, Mott-driven bec-bcs crossover in a doped spin liquid candidate κ -(BEDT-TTF)₄hg_{2.89}br₈, *Phys. Rev. X* **12**, 011016 (2022).
- [50] P. Zhou, L. Chen, Y. Liu, I. Sochnikov, A. T. Bollinger, M.-G. Han, Y. Zhu, X. He, I. Božović, and D. Natelson, Electron pairing in the pseudogap state revealed by shot noise in copper oxide junctions, *Nature* **572**, 493 (2019).
- [51] I. Božović and J. Levy, Pre-formed cooper pairs in copper oxides and laalo 3—srtio 3 heterostructures, *Nature Physics* **16**, 712 (2020).
- [52] K. M. Bastiaans, D. Chatzopoulos, J.-F. Ge, D. Cho, W. O. Tromp, J. M. van Ruitenbeek, M. H. Fischer, P. J. de Visser, D. J. Thoen, E. F. C. Driessen, T. M. Klapwijk, and M. P. Allan, Direct evidence for cooper pairing without a spectral gap in a disordered superconductor above t_c , *Science* **374**, 608 (2021), <https://www.science.org/doi/pdf/10.1126/science.abe3987>.
- [53] X. Han, B. Liu, and J. Hu, Enhancement of the thermal-transport figure of merit and breakdown of the wiedemann-franz law in unitary fermi gases, *Phys. Rev. A* **100**, 043604 (2019).
- [54] T. Sowiński, M. Gajda, and K. Rzażewski, Diffusion in a system of a few distinguishable fermions in a one-dimensional double-well potential, *EPL (Europhysics Letters)* **113**, 56003 (2016).
- [55] J. Erdmann, S. I. Mistakidis, and P. Schmelcher, Correlated tunneling dynamics of an ultracold fermi-fermi mixture confined in a double well, *Phys. Rev. A* **98**, 053614 (2018).
- [56] Supplement, See Supporting Information Appendix for a detailed information on detailed calculation of a current and noise, the single-particle Green's function at dilute limit, and effect of the tunneling-coupling ratio.
- [57] D. J. Griffiths and D. F. Schroeter, *Introduction to quantum mechanics* (Cambridge university press, 2018).
- [58] We note that the validity of the truncation with respect to the lowest-order tunneling coupling was confirmed in the recent experiment [7].
- [59] M. Büttiker, Scattering theory of current and intensity noise correlations in conductors and wave guides, *Phys. Rev. B* **46**, 12485 (1992).
- [60] Y. M. Blanter and M. Büttiker, Shot noise in mesoscopic conductors, *Physics reports* **336**, 1 (2000).
- [61] Y. Imry, *Introduction to mesoscopic physics*, 2 (Oxford University Press on Demand, 2002).
- [62] H. Bouchiat, Y. Gefen, S. Guéron, G. Montambaux, and J. Dalibard, *Nanophysics: Coherence and Transport: Lecture Notes of the Les Houches Summer School 2004* (Elsevier, 2005).
- [63] O. S. Lumbroso, L. Simine, A. Nitzan, D. Segal, and O. Tal, Electronic noise due to temperature differences in atomic-scale junctions, *Nature* **562**, 240 (2018).
- [64] V. Ngampruetikorn, M. M. Parish, and J. Levinsen, High-temperature limit of the resonant fermi gas, *Phys. Rev. A* **91**, 013606 (2015).
- [65] W. Zwerger, *The BCS-BEC crossover and the unitary Fermi gas*, Vol. 836 (Springer Science & Business Media, 2011).
- [66] P. Pieri and G. C. Strinati, Strong-coupling limit in the evolution from bcs superconductivity to bose-einstein condensation, *Phys. Rev. B* **61**, 15370 (2000).
- [67] N. Andrenacci, P. Pieri, and G. C. Strinati, Evolution from bcs superconductivity to bose-einstein condensation: Current correlation function in the broken-symmetry phase, *Phys. Rev. B* **68**, 144507 (2003).
- [68] Here, “BEC regime” is used for the regime where the two-body attraction is so strong that the associated superfluid state behaves like molecular BEC below T_c [38, 39]. In this regard, the strongly-attractive regime even above T_c is also referred as to the BEC regime for characterizing the interaction strength.
- [69] We note that in this regime the numerical cost is large due to the overlap of Bose distribution function and sharp peaks in $\mathcal{B}_{q,L,R}$. We confirmed that the qualitative behavior is robust against the accuracy of the frequency integration.
- [70] M. Jarrell and J. Gubernatis, Bayesian inference and the analytic continuation of imaginary-time quantum monte carlo data, *Physics Reports* **269**, 133 (1996).
- [71] X.-J. Liu, Virial expansion for a strongly correlated fermi system and its application to ultracold atomic fermi gases, *Physics Reports* **524**, 37 (2013), virial expansion for a strongly correlated Fermi system and its application to ultracold atomic Fermi gases.
- [72] Y. Sagi, T. E. Drake, R. Paudel, and D. S. Jin, Measurement of the homogeneous contact of a unitary fermi gas, *Phys. Rev. Lett.* **109**, 220402 (2012).

PAIR-TUNNELING COUPLING

Following Ref. [25], we obtain the renormalized pair-tunneling coupling as

$$\mathcal{T}_{2,\text{ren.}} \equiv \frac{\Lambda^2 k_{\text{F,L}}}{3\sqrt{2}\pi^2} \mathcal{T}_2 \simeq \frac{\Lambda^2 k_{\text{F,L}}}{3\sqrt{2}\pi^2} 2|g| \text{Re}[B_{0,\uparrow} B_{0,\downarrow}] \quad (10)$$

where $B_{0,\sigma}$ is the amplitude of the transmitted wave with respect to the potential barrier. Since we consider the spin-balanced system, we take $B_{0,\uparrow} = B_{0,\downarrow} \equiv B_0$. Near unitarity ($a^{-1} \simeq 0$), g can be rewritten as $g = \frac{4\pi a}{m} \frac{1}{1 - \frac{4\pi a}{m} \frac{m\Lambda}{2\pi^2}} \simeq -\frac{2\pi^2}{m\Lambda}$. While g is negative, $\mathcal{T}_{2,\text{ren.}}$ can be taken to be positive by the appropriate gauge transformation. In the case of the delta potential barrier $V(x) = V_0 \delta(x/\ell)$ being perpendicular to the x axis (ℓ is the typical length scale of the tunneling region, e.g., the width of the actual potential barrier), which is given by a constant $V(\mathbf{k}) = V_0$ in the momentum space, we find [57]

$$\text{Re}[B_0^2] \simeq T_{\text{trans.}} = \frac{1}{1 + \frac{mV_0^2 \ell^2}{2E_{\text{F,L}}}}, \quad (11)$$

where $T_{\text{trans.}}$ is the transmission coefficient. For simplicity, we take $E_{\text{F,L}}$ for the energy of the incident particle and the transverse motion along the barrier is neglected. Combining them, we get

$$\mathcal{T}_{2,\text{ren.}} \simeq \frac{4\Lambda k_{\text{F,L}}}{3\sqrt{2}m} \frac{1}{1 + \frac{mV_0^2 \ell^2}{2E_{\text{F,L}}}}. \quad (12)$$

In turn, we obtain the quasiparticle-tunneling coupling \mathcal{T}_1 as

$$\mathcal{T}_1 \simeq B_0(E_{\text{F,L}} + V_0) \equiv \frac{E_{\text{F,L}} + V_0}{\sqrt{1 + \frac{mV_0^2 \ell^2}{2E_{\text{F,L}}}}}, \quad (13)$$

where we ignore the higher order term involving the reflection amplitude. Note that the Hartree term gN_{L} is negligible compared to the other term for the present short-range interaction. In this way, we obtain

$$\frac{\mathcal{T}_{2,\text{ren.}}}{\mathcal{T}_1} \simeq \frac{4}{3\sqrt{2}} \frac{\Lambda k_{\text{F,L}}}{m(E_{\text{F,L}} + V_0)} \frac{1}{\sqrt{1 + \frac{mV_0^2 \ell^2}{2E_{\text{F,L}}}}} \equiv \frac{8}{3\sqrt{2}} \frac{\Lambda/k_{\text{F,L}}}{\left(1 + \frac{V_0}{E_{\text{F,L}}}\right) \sqrt{1 + \left(\frac{V_0}{E_{\text{F,L}}}\right)^2 (k_{\text{F,L}}\ell)^2}}. \quad (14)$$

While we use the contact-type interaction with the cutoff regularization, the cutoff Λ can be associated with the effective range r_{eff} as $r_{\text{eff}} = \frac{4}{\pi\Lambda}$ (and moreover the interaction range $r_{\text{int.}}$) [39]. In cold atom experiments, the typical interaction range is approximately given by $|k_{\text{F,L}} r_{\text{int.}}| \simeq 10^{-2}$ [2, 72].

Figure 5 shows $\mathcal{T}_{2,\text{ren.}}/\mathcal{T}_1$ in Eq. (14) as a function of $V_0/E_{\text{F,L}}$ at different $k_{\text{F,L}}\ell$. One can see that the ratio can be tuned by changing V_0 .

SCHWINGER-KELDYSH APPROACH FOR CURRENT AND NOISE

We start from the current operator given by

$$\hat{I} = \hat{I}_{\text{qp}} + \hat{I}_{\text{pair}}, \quad (15)$$

$$\hat{I}_{\text{qp}} = i \sum_{\mathbf{p}, \mathbf{k}, \sigma} t_{\mathbf{k}, \mathbf{p}} \left[c_{\mathbf{k}, \sigma, \text{L}}^\dagger c_{\mathbf{p}, \sigma, \text{R}} - c_{\mathbf{p}, \sigma, \text{R}}^\dagger c_{\mathbf{k}, \sigma, \text{L}} \right], \quad (16)$$

$$\hat{I}_{\text{pair}} = 2i \sum_{\mathbf{q}, \mathbf{q}'} w_{\mathbf{q}, \mathbf{q}'} \left[P_{\mathbf{q}, \text{L}}^\dagger P_{\mathbf{q}', \text{R}} - P_{\mathbf{q}', \text{R}}^\dagger P_{\mathbf{q}, \text{L}} \right], \quad (17)$$

where \hat{I}_{qp} and \hat{I}_{pair} are operators for quasiparticle and pair currents, respectively. Truncating the higher-order contributions with respect to the tunneling Hamiltonians [i.e., $O(H_{1\text{T}}^3)$, $O(H_{2\text{T}}^3)$], we can evaluate their expectation

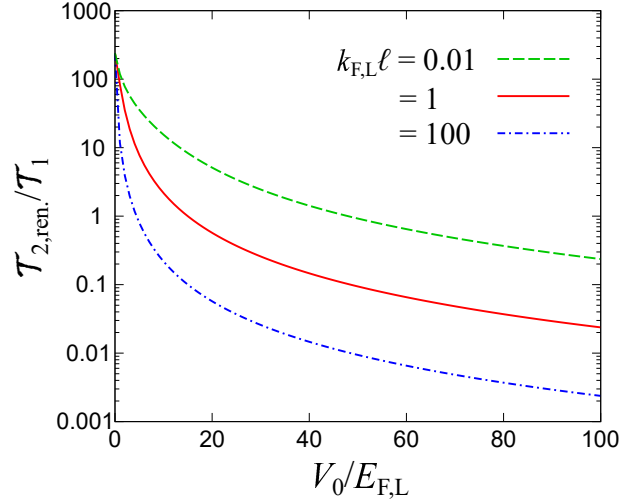


FIG. 5. The dimensionless ratio between $\mathcal{T}_{2,\text{ren.}}$ and \mathcal{T}_1 given by (14), where we used $k_{F,L}r_{\text{eff}} = 10^{-2}$. V_0 and ℓ are defined through the delta-function form of the potential barrier $V(x) = V_0\delta(x/\ell)$.

values, $I_{\text{qp}}(t_1, t_2) = \langle \Psi(t_1) | \hat{I}_{\text{qp}} | \Psi(t_2) \rangle$ and $I_{\text{pair}}(t_1, t_2) = \langle \Psi(t_1) | \hat{I}_{\text{pair}} | \Psi(t_2) \rangle$, for the different times t_1 and t_2 , where $|\Psi(t)\rangle$ is the state-vector of the steady state. First, the quasiparticle contribution reads

$$I_{\text{qp}}(t_1, t_2) = -2 \int_C dt' \sum_{\mathbf{p}, \mathbf{k}, \sigma} |t_{\mathbf{k}, \mathbf{p}}|^2 \text{Re} \left[\langle T_C c_{\mathbf{k}, \sigma, \text{R}}(t_2) c_{\mathbf{k}, \sigma, \text{R}}^\dagger(t') \rangle \langle T_C c_{\mathbf{p}, \sigma, \text{L}}(t') c_{\mathbf{p}, \sigma, \text{L}}^\dagger(t_1) \rangle \right], \quad (18)$$

where C denotes the Keldysh contour. Note that while the right hand side of Eq. (18) depends only on $t_1 - t_2$ in considering the steady state. Using the Green's functions, we rewrite $I_{\text{qp}}(t_1, t_2)$ as

$$I_{\text{qp}}(t_1, t_2) = 2 \int_{-\infty}^{\infty} dt' \sum_{\mathbf{p}, \mathbf{k}, \sigma} |t_{\mathbf{k}, \mathbf{p}}|^2 \text{Re} \left[G_{\mathbf{p}, \text{R}}^{\text{ret.}}(t_2 - t') G_{\mathbf{k}, \text{L}}^<(t' - t_1) + G_{\mathbf{p}, \text{R}}^<(t_2 - t') G_{\mathbf{k}, \text{L}}^{\text{adv.}}(t' - t_1) \right], \quad (19)$$

where $G^{\text{ret. (adv.)}}$ is the retarded (advanced) Green's function of a fermion in thermal equilibrium. The lesser component $G^<$ contains the information of the thermal distribution in each reservoir. Here, we take $t_1 = t_2 \equiv t$ and the Fourier transformation

$$I_{\text{qp}} = 2 \int \frac{d\omega}{2\pi} \sum_{\mathbf{p}, \mathbf{k}, \sigma} |t_{\mathbf{k}, \mathbf{p}}|^2 \text{Re} \left[G_{\mathbf{p}, \text{R}}^{\text{ret.}}(\omega) G_{\mathbf{k}, \text{L}}^<(\omega) + G_{\mathbf{p}, \text{R}}^<(\omega) G_{\mathbf{k}, \text{L}}^{\text{ret.*}}(\omega) \right]. \quad (20)$$

Moreover, we use

$$G_{\mathbf{k}, \text{j}}^<(\omega) = -2i f_{\text{j}}(\omega) \text{Im} G_{\mathbf{k}, \text{j}}^{\text{ret.*}}(\omega) \equiv i f_{\text{j}}(\omega) \mathcal{A}_{\mathbf{k}, \text{j}}(\omega), \quad (21)$$

where

$$f_{\text{j}}(\omega) = \frac{1}{\exp(\frac{\omega - \mu_{\text{j}}}{T_{\text{j}}}) + 1} \quad (22)$$

is the Fermi-Dirac distribution function. We use Matsubara Green's functions in each reservoir reaching thermal equilibrium as a grand-canonical ensemble with $-\mu_{\text{j}} \hat{N}_{\text{j}}$ and obtain the retarded(advanced) Green's function by the analytic continuation with μ_{j} as $i\omega_n \rightarrow \omega + i\eta - \mu_{\text{j}}$ in each reservoir. Then, we obtain

$$I_{\text{qp}} = \int \frac{d\omega}{2\pi} \sum_{\mathbf{p}, \mathbf{k}, \sigma} |t_{\mathbf{k}, \mathbf{p}}|^2 \mathcal{A}_{\mathbf{p}, \text{L}}(\omega) \mathcal{A}_{\mathbf{k}, \text{R}}(\omega) [f_{\text{L}}(\omega) - f_{\text{R}}(\omega)]. \quad (23)$$

Similarly, we obtain the pair current contribution as

$$I_{\text{pair}} = 2 \sum_{\mathbf{q}, \mathbf{q}'} \int \frac{d\omega}{2\pi} |\omega_{\mathbf{q}, \mathbf{q}'}|^2 \mathcal{B}_{\mathbf{q}, \text{L}}(\omega) \mathcal{B}_{\mathbf{q}', \text{R}}(\omega) [b_{\text{L}}(\omega) - b_{\text{R}}(\omega)], \quad (24)$$

where we used the relation for the two-particle Green's function given $\mathcal{G}^<$ by

$$\mathcal{G}_{q,j}^<(\omega) = 2ib_j(\omega) \text{Im} \mathcal{G}_{q,j}^{\text{ret.}}(\omega) \equiv -ib_j(\omega) \mathcal{B}_{q,j}(\omega), \quad (25)$$

and the Bose-Einstein distribution function

$$b_j(\omega) = \frac{1}{\exp\left(\frac{\omega - \mu_{b,j}}{T_j}\right) - 1}, \quad (26)$$

with a bosonic (pair) chemical potential $\mu_{b,j} = 2\mu_j$. $\mathcal{G}^{<(>)}$ and $\mathcal{G}^{\text{ret.}(\text{adv.})}$ are the lesser (greater) and retarded (advanced) components of two-particle Green's functions, respectively. One can find that $I = I_{\text{qp}} + I_{\text{pair}}$ obtained from Eqs. (23) and (24) is equivalent to Eq. (4) in the main text. We briefly note that one may find the correlation between quasiparticle and tunneling currents in the higher-order contributions such as the term proportional to $t_{\mathbf{k},\mathbf{p}}^2 w_{\mathbf{q},\mathbf{q}'}$, which is beyond the scope in this work.

Next, we consider the current noise

$$\mathcal{S} = \frac{1}{2} \int_{-\infty}^{\infty} dt \left(\langle \hat{I}(t) \hat{I}(0) \rangle + \langle \hat{I}(0) \hat{I}(t) \rangle \right). \quad (27)$$

At lowest order of tunneling couplings, we obtain

$$\begin{aligned} \langle \hat{I}(t) \hat{I}(0) \rangle &= \sum_{\mathbf{p}, \mathbf{k}, \sigma} |t_{\mathbf{p}, \mathbf{k}}|^2 \left[G_{\mathbf{k}, \text{L}}^<(t) G_{\mathbf{p}, \text{R}}^>(-t) + G_{\mathbf{p}, \text{R}}^<(t) G_{\mathbf{k}, \text{L}}^>(-t) \right] \\ &\quad - 4 \sum_{\mathbf{q}, \mathbf{q}'} |w_{\mathbf{q}, \mathbf{q}'}|^2 \left[\mathcal{G}_{\mathbf{q}, \text{L}}^<(t) \mathcal{G}_{\mathbf{q}', \text{R}}^>(-t) + \mathcal{G}_{\mathbf{q}', \text{R}}^<(t) \mathcal{G}_{\mathbf{q}, \text{L}}^>(-t) \right], \end{aligned} \quad (28)$$

$$\begin{aligned} \langle \hat{I}(0) \hat{I}(t) \rangle &= \sum_{\mathbf{p}, \mathbf{k}, \sigma} |t_{\mathbf{p}, \mathbf{k}}|^2 \left[G_{\mathbf{k}, \text{L}}^<(-t) G_{\mathbf{p}, \text{R}}^>(t) + G_{\mathbf{p}, \text{R}}^<(-t) G_{\mathbf{k}, \text{L}}^>(t) \right] \\ &\quad - 4 \sum_{\mathbf{q}, \mathbf{q}'} |w_{\mathbf{q}, \mathbf{q}'}|^2 \left[\mathcal{G}_{\mathbf{q}, \text{L}}^<(-t) \mathcal{G}_{\mathbf{q}', \text{R}}^>(t) + \mathcal{G}_{\mathbf{q}', \text{R}}^<(-t) \mathcal{G}_{\mathbf{q}, \text{L}}^>(t) \right]. \end{aligned} \quad (29)$$

Collecting them and taking the Fourier transformation, we obtain

$$\begin{aligned} \mathcal{S} &= \mathcal{S}_{\text{qp}} + \mathcal{S}_{\text{pair}}, \\ \mathcal{S}_{\text{qp}} &= \int_{-\infty}^{\infty} \frac{d\omega}{2\pi} \sum_{\mathbf{k}, \mathbf{p}, \sigma} |t_{\mathbf{k}, \mathbf{p}, \sigma}|^2 \left[G_{\mathbf{k}, \text{L}}^<(\omega) G_{\mathbf{p}, \text{R}}^>(\omega) + G_{\mathbf{k}, \text{L}}^>(\omega) G_{\mathbf{p}, \text{R}}^<(\omega) \right], \\ \mathcal{S}_{\text{pair}} &= -4 \int_{-\infty}^{\infty} \frac{d\omega}{2\pi} \sum_{\mathbf{q}, \mathbf{q}'} |w_{\mathbf{q}, \mathbf{q}'}|^2 \left[\mathcal{G}_{\mathbf{q}, \text{L}}^<(\omega) \mathcal{G}_{\mathbf{q}', \text{R}}^>(\omega) + \mathcal{G}_{\mathbf{q}, \text{L}}^>(\omega) \mathcal{G}_{\mathbf{q}', \text{R}}^<(\omega) \right]. \end{aligned} \quad (30)$$

Using the relations associated with greater Green's functions

$$G_{\mathbf{p}, j}^>(\omega) = -i\mathcal{A}_{\mathbf{p}, j}(\omega)[1 - f_j(\omega)], \quad \mathcal{G}_{\mathbf{q}, j}^>(\omega) = -i\mathcal{B}_{\mathbf{q}, j}(\omega)[1 + b_j(\omega)], \quad (32)$$

and the lesser ones given by Eqs. (21) and (25), we obtain

$$\begin{aligned} \mathcal{S}_{\text{qp}} &= \int_{-\infty}^{\infty} \frac{d\omega}{2\pi} \sum_{\mathbf{k}, \mathbf{p}, \sigma} |t_{\mathbf{k}, \mathbf{p}, \sigma}|^2 \mathcal{A}_{\mathbf{k}, \text{L}}(\omega) \mathcal{A}_{\mathbf{p}, \text{R}}(\omega) [f_{\text{L}}(\omega) \{1 - f_{\text{R}}(\omega)\} + \{1 - f_{\text{L}}(\omega)\} f_{\text{R}}(\omega)] \\ \mathcal{S}_{\text{pair}} &= 4 \int_{-\infty}^{\infty} \frac{d\omega}{2\pi} \sum_{\mathbf{q}, \mathbf{q}'} |w_{\mathbf{q}, \mathbf{q}'}|^2 \mathcal{B}_{\mathbf{q}, \text{L}}(\omega) \mathcal{B}_{\mathbf{q}', \text{R}}(\omega) [b_{\text{L}}(\omega) \{1 + b_{\text{R}}(\omega)\} + b_{\text{R}}(\omega) \{1 + b_{\text{L}}(\omega)\}], \end{aligned} \quad (33)$$

which is equivalent to Eq. (6) in the main text. We note that, in (33), the terms proportional to $[f_j(\omega) \{1 - f_j(\omega)\}]$ and $[b_j(\omega) \{1 + b_j(\omega)\}]$ ($j = \text{L}, \text{R}$) do not appear in contrast to Ref. [60] because we consider the lowest-order contributions $O(t_{\mathbf{k}, \mathbf{p}, \sigma}^2)$ and $O(w_{\mathbf{q}, \mathbf{q}'}^2)$ without the reflection term. Moreover, the correlation of two noises may appear in the higher-order contributions [e.g., $O(t_{\mathbf{k}, \mathbf{p}, \sigma}^2 w_{\mathbf{q}, \mathbf{q}'})$], which will be considered in the future work. For a small bias limit at equal temperatures $T_{\text{L}} = T_{\text{R}} \equiv T$ where $\Delta\mu \rightarrow 0$ and $f_{\text{R}}(\omega) \rightarrow f_{\text{L}}(\omega) \equiv f(\omega)$ with $\mu_{\text{R}} \rightarrow \mu_{\text{L}} \equiv \mu$, we obtain

$$f_{\text{L}}(\omega) - f_{\text{R}}(\omega) = -\frac{\partial f(\omega)}{\partial \omega} \Delta\mu + O((\Delta\mu)^2), \quad (34)$$

$$b_L(\omega) - b_R(\omega) = -2 \frac{\partial b(\omega)}{\partial \omega} \Delta\mu + O((\Delta\mu)^2). \quad (35)$$

Using

$$f(\omega)\{1 - f(\omega)\} = -T \frac{\partial f(\omega)}{\partial \omega}, \quad b(\omega)\{1 + b(\omega)\} = -T \frac{\partial b(\omega)}{\partial \omega}, \quad (36)$$

we recover the Onsager's relation

$$\mathcal{S}(\Delta\mu \rightarrow 0) = 2T \frac{I}{\Delta\mu}. \quad (37)$$

Moreover, the current and the noise can be rewritten as

$$I_{\text{qp}} = \int_{-\infty}^{\infty} \frac{d\omega}{2\pi} \sum_{\mathbf{p}, \mathbf{k}, \sigma} |t_{\mathbf{k}, \mathbf{p}}|^2 \mathcal{A}_{\mathbf{k}, \text{L}}(\omega) \mathcal{A}_{\mathbf{p}, \text{R}}(\omega) \left[-\frac{1}{2} \frac{\sinh\left(\frac{\beta_L(\omega - \mu_L) - \beta_R(\omega - \mu_R)}{2}\right)}{\cosh\left(\frac{\beta_L(\omega - \mu_L)}{2}\right) \cosh\left(\frac{\beta_R(\omega - \mu_R)}{2}\right)} \right], \quad (38)$$

$$I_{\text{pair}} = 2 \int_{-\infty}^{\infty} \frac{d\omega}{2\pi} \sum_{\mathbf{q}, \mathbf{q}'} |w_{\mathbf{q}, \mathbf{q}'}|^2 \mathcal{B}_{\mathbf{q}, \text{L}}(\omega) \mathcal{B}_{\mathbf{q}', \text{R}}(\omega) \left[-\frac{1}{2} \frac{\sinh\left(\frac{\beta_{\text{b}, \text{L}}(\omega - \mu_{\text{b}, \text{L}}) - \beta_{\text{b}, \text{R}}(\omega - \mu_{\text{b}, \text{R}})}{2}\right)}{\sinh\left(\frac{\beta_{\text{b}, \text{L}}(\omega - \mu_{\text{b}, \text{L}})}{2}\right) \sinh\left(\frac{\beta_{\text{b}, \text{R}}(\omega - \mu_{\text{b}, \text{R}})}{2}\right)} \right], \quad (39)$$

$$\mathcal{S}_{\text{qp}} = \int_{-\infty}^{\infty} \frac{d\omega}{2\pi} \sum_{\mathbf{k}, \mathbf{p}, \sigma} |t_{\mathbf{k}, \mathbf{p}}|^2 \mathcal{A}_{\mathbf{k}, \text{L}}(\omega) \mathcal{A}_{\mathbf{p}, \text{R}}(\omega) \left[-\frac{1}{2} \frac{\cosh\left(\frac{\beta_L(\omega - \mu_L) - \beta_R(\omega - \mu_R)}{2}\right)}{\cosh\left(\frac{\beta_L(\omega - \mu_L)}{2}\right) \cosh\left(\frac{\beta_R(\omega - \mu_R)}{2}\right)} \right], \quad (40)$$

$$\mathcal{S}_{\text{pair}} = 4 \int_{-\infty}^{\infty} \frac{d\omega}{2\pi} \sum_{\mathbf{q}, \mathbf{q}'} |w_{\mathbf{q}, \mathbf{q}'}|^2 \mathcal{B}_{\mathbf{q}, \text{L}}(\omega) \mathcal{B}_{\mathbf{q}', \text{R}}(\omega) \left[-\frac{1}{2} \frac{\cosh\left(\frac{\beta_{\text{b}, \text{L}}(\omega - \mu_{\text{b}, \text{L}}) - \beta_{\text{b}, \text{R}}(\omega - \mu_{\text{b}, \text{R}})}{2}\right)}{\sinh\left(\frac{\beta_{\text{b}, \text{L}}(\omega - \mu_{\text{b}, \text{L}})}{2}\right) \sinh\left(\frac{\beta_{\text{b}, \text{R}}(\omega - \mu_{\text{b}, \text{R}})}{2}\right)} \right]. \quad (41)$$

In particular, considering the large-biased limit where

$$\tanh\left(\frac{\beta_L(\omega - \mu_L) - \beta_R(\omega - \mu_R)}{2}\right) \simeq \tanh\left(\frac{\beta_L(\omega - \mu_{\text{b}, \text{L}}) - \beta_R(\omega - \mu_{\text{b}, \text{R}})}{2}\right) \simeq 1, \quad (42)$$

is satisfied, we obtain

$$\mathcal{S}_{\text{qp}}(\Delta\mu \rightarrow \infty) \rightarrow I_{\text{qp}}, \quad \mathcal{S}_{\text{pair}}(\Delta\mu \rightarrow \infty) \rightarrow 2I_{\text{pair}}, \quad (43)$$

where we have denoted $I \equiv I_{\text{qp}} + I_{\text{pair}}$. The result of Eq. (43) motivates us to consider the Fano factor

$$F = \frac{\mathcal{S}}{I} = \frac{\mathcal{S}_{\text{qp}} + \mathcal{S}_{\text{pair}}}{I_{\text{qp}} + I_{\text{pair}}}. \quad (44)$$

Then, one can see that the Fano factor F in a large-biased junction changes from 1 to 2 reflecting the ratio between I_{qp} and I_{pair} .

MANY-BODY T -MATRIX APPROXIMATION

To demonstrate this, we employ the many-body TMA to calculate spectral functions $\mathcal{A}_{\mathbf{k}, \text{j}}(\omega)$, $\mathcal{B}_{\mathbf{q}, \text{j}}(\omega)$, and μ_{j} for given densities N_{j} in the BCS-BEC crossover regime [39]. The single-particle propagator is given by

$$G_{\mathbf{k}, \text{j}}(i\omega_n) = \frac{1}{G_{\mathbf{k}, \text{j}}^0(i\omega_n)^{-1} - \Sigma_{\mathbf{k}, \text{j}}(i\omega_n)}, \quad (45)$$

$$\Sigma_{\mathbf{k}, \text{j}}(i\omega_n) = T_{\text{j}} \sum_{\mathbf{q}, \ell} \Gamma_{\mathbf{q}, \text{j}}(i\nu_{\ell}) G_{\mathbf{q} - \mathbf{k}, \text{j}}^0(i\nu_{\ell} - i\omega_n), \quad (46)$$

where $G_{\mathbf{k},j}^0(i\omega_n) = (i\omega_n - \xi_{\mathbf{k},j})^{-1}$ denotes the bare propagator and $\Sigma_{\mathbf{k},j}(i\omega_n)$ denotes the TMA self-energy. Following a standard TMA procedure [65], the T -matrix $\Gamma_{\mathbf{q},j}(i\nu_\ell)$ is formulated by incorporating the particle-particle multiple scattering as

$$\Gamma_{\mathbf{q},j}(i\nu_\ell) = g [1 - g\Pi_{\mathbf{q},j}(i\nu_\ell)]^{-1}, \quad (47)$$

using the bare two-body propagator given as

$$\Pi_{\mathbf{q},j}(i\nu_\ell) = -T_j \sum_{\mathbf{p},n} G_{\mathbf{p}+\mathbf{q}/2,j}^0(i\omega_n + i\nu_\ell) G_{-\mathbf{p}+\mathbf{q}/2,j}^0(-i\omega_n). \quad (48)$$

The fermion (boson) Matsubara frequency is denoted by ω_n (ν_ℓ). Furthermore, we define the dressed two-body propagator [66] as

$$\mathcal{G}_{\mathbf{q},j}(i\nu_\ell) = \Pi_{\mathbf{q},j}(i\nu_\ell) [1 + \Pi_{\mathbf{q},j}(i\nu_\ell)\Gamma_{\mathbf{q},j}(i\nu_\ell)]. \quad (49)$$

The spectral functions can be obtained from the analytic continuation as $\mathcal{A}_{\mathbf{k},j}(\omega) = -2 \text{Im} G_{\mathbf{k},j}(i\omega_n \rightarrow \omega - \mu_j + i\eta)$ and $\mathcal{B}_{\mathbf{q},j}(\omega) = -2 \text{Im} \mathcal{G}_{\mathbf{q},j}(i\nu_\ell \rightarrow \omega - \mu_{b,j} + i\eta)$ with an infinitesimal small number η .

RETARDED PROPAGATORS IN THE DILUTE RESERVOIR

For the single-particle Green's function in the reservoir R at dilute limit, we employ the non-interacting one given by

$$G_{\mathbf{p},R}^{\text{ret.}}(\omega) = \frac{1}{\omega + i\eta - \epsilon_{\mathbf{p}}}, \quad (50)$$

where the self-energy correction is ignored [noting $\epsilon_{\mathbf{p}} = p^2/(2m)$]. For the two-body sector, we can rewrite the lowest-order two-body propagator as

$$\Pi_{\mathbf{q},j}^{\text{ret.}}(\omega) \equiv \Pi_{\mathbf{q},0}(\omega) + \Xi_{\mathbf{q},j}(\omega), \quad (51)$$

where

$$\Pi_{\mathbf{q},0}(\omega) = \sum_{\mathbf{p}} \frac{1}{\omega + i\eta - \epsilon_{\mathbf{p}+\mathbf{q}/2} - \epsilon_{-\mathbf{p}+\mathbf{q}/2}} \quad (52)$$

and

$$\Xi_{\mathbf{q},j}(\omega) = - \sum_{\mathbf{p}} \frac{f_j(\epsilon_{\mathbf{p}+\mathbf{q}/2}) + f_j(\epsilon_{-\mathbf{p}+\mathbf{q}/2})}{\omega + i\eta - \epsilon_{\mathbf{p}+\mathbf{q}/2} - \epsilon_{-\mathbf{p}+\mathbf{q}/2}} \quad (53)$$

are the in-vacuum two-body Green's function and the medium correction, respectively (for more details, see e.g., Refs. [38, 39]). Taking $\alpha^2 = q^2/4 - m\omega - i\delta$, we can analytically obtain

$$\Pi_{\mathbf{q},0}(\omega) = -\frac{m\Lambda}{2\pi^2} + \frac{m\alpha}{2\pi^2} \tan^{-1} \left(\frac{\Lambda}{\alpha} \right), \quad (54)$$

where Λ is an ultraviolet cutoff. Note that Λ is renormalized via

$$\frac{m}{4\pi a} = \frac{1}{g} + \frac{m\Lambda}{2\pi^2}, \quad (55)$$

which leads to

$$\begin{aligned} \frac{1}{\Gamma_{\mathbf{q},j}^{\text{ret.}}(\omega)} &= \frac{m}{4\pi a} - \Pi_{\mathbf{q},j}^{\text{ret.}}(\omega) - \frac{m\Lambda}{2\pi^2} \\ &\simeq \frac{m}{4\pi a} - \Xi_{\mathbf{q}}(\omega) - \frac{m\alpha}{4\pi} \end{aligned} \quad (56)$$

where the ultraviolet divergence is cancelled ($\tan^{-1}(\frac{\Lambda}{\alpha}) \simeq \pi/2$ is used in the second line).

In the dilute limit, the fermionic medium correction $\Xi_{q,R}(\omega)$ is negligible. In this case, one can approximately obtain

$$\mathcal{G}_{q,R}^{\text{ret.}}(\omega) \simeq \Pi_{q,0}(\omega) [1 - g\Pi_{q,0}(\omega)]^{-1}. \quad (57)$$

where $\mathcal{G}_{q,R}^{\text{ret.}}(\omega)$ does not involve any poles on the real frequency axis (i.e. bound states) at $a^{-1} < 0$. Note that the two-body continuum exists above $\omega = q^2/(4m)$. In the weak-coupling side ($a < 0$), we obtain

$$\mathcal{B}_{q,R}(\omega) = -2 \text{Im} \mathcal{G}_{q,R}^{\text{ret.}}(\omega) = 0. \quad (\omega < q^2/4m). \quad (58)$$

Simultaneously, the frequency integration is restricted as $\omega > 0$. This fact indicates that particles in the reservoir L are transferred to the two-body continuum in the reservoir R via the two-body tunneling process in the weak-coupling side ($a < 0$). On the other hand, in the strong-coupling limit ($a \rightarrow +\infty$), we obtain [66, 67]

$$\mathcal{G}_{q,R}^{\text{ret.}}(\omega) \simeq \left(\frac{m\Lambda}{2\pi^2}\right)^2 \frac{8\pi}{m^2 a} \frac{1}{\omega + i\eta - \frac{q^2}{4m} + E_b} \quad (\Lambda \rightarrow \infty), \quad (59)$$

which is proportional to the bosonic Green's function of a bound molecule with the binding energy $E_b = 1/(ma^2)$. Thus, in the strong-coupling regime ($a > 0$), particles in the reservoir L can be transferred to the molecular bound states in the reservoir R via the two-body tunneling process.

LARGE-BIAS LIMIT

In the main text, we considered a situation where fermions in the strongly-correlated reservoir L with a finite density N_L go through the tunneling junction to the dilute reservoir R with a vanishing density $N_R \rightarrow 0$, i.e., $\mu_R \rightarrow -\infty$. While we take the same temperatures $T_L = T_R$ in the two reservoirs, T_R does not affect the result in the present case of $\mu_R \rightarrow -\infty$ because the fugacity $z_R = e^{\mu_R/T_R}$ characterizing the distribution vanishes regardless of the value of T_R . The condition of the large bias limit [$\mu_R = T_R \ln(z_R) \rightarrow -\infty$] is unchanged in both BCS and BEC sides at nonzero temperatures because the dilute reservoir R obeys the Boltzmann statistics. Indeed, we obtain vanishing N_R as [64]

$$N_R = 2z_R \left(\frac{2\pi}{mT_R}\right)^{\frac{3}{2}} + O(z_R^2) \rightarrow 0 \quad (z_R \rightarrow 0). \quad (60)$$

The number density N_L of the L-reservoir can be numerically obtained from

$$N_L = T_L \sum_{\mathbf{p}, \sigma, n} G_{\mathbf{p},L}(i\omega_n). \quad (61)$$

In this regard, we normalize physical quantities by using the Fermi energy $E_{F,L} = (3\pi^2 N_L)^{\frac{2}{3}}/(2m)$ and momentum $k_{F,L} = (3\pi^2 N_L)^{\frac{1}{3}}$.

While the Fano factor is well described by the Onsager's relation $F^{-1}(\Delta\mu \rightarrow 0) = \frac{\Delta\mu}{2T}$ in the low-bias regime, F^{-1} approaches the large-bias limit ($\mu_R \rightarrow -\infty$) when $\Delta\mu/E_{F,L} \gtrsim 1$. This indicates that it is sufficient to reach the large-bias limit when $\Delta\mu$ is larger than the many-body scale of the reservoir, that is, $E_{F,L}$. We note that $\Delta\mu$ can be controllable in cold atomic experiments by preparing the reservoirs with the large density imbalance.

I. DIFFERENT TUNNELING-COUPLING RATIO

Figure 6 shows the calculated Fano factor F with different tunneling-coupling ratio $\mathcal{T}_{2,\text{ren.}}/\mathcal{T}_1$ in the entire BCS-BEC crossover regime at $T_L/T_{F,L} = 0.3$. While in the main text we employed $\mathcal{T}_{2,\text{ren.}}/\mathcal{T}_1 = 1$, this ratio depends on the actual detailed setups in each experiment. If the two-body tunneling is relatively strong as $\mathcal{T}_{2,\text{ren.}}/\mathcal{T}_1 = 10$, F is close to 2 even in the weak-coupling side [$(k_{F,L}a)^{-1} \simeq -1$]. However, F decreases at weaker coupling even in this case. On the other hand, in the case with $\mathcal{T}_{2,\text{ren.}}/\mathcal{T}_1 = 0.1$, F remains to be close to 1 even around unitarity. Nevertheless, F rapidly increases around $(k_{F,L}a)^{-1} = 0.3$ and consequently reaches $F = 2$ in the strong-coupling limit.

In this way, the detailed structure of the tunneling junction affects how F increases in the BCS-BEC crossover regime. However, our conclusion that $F = 1$ and $F = 2$ are achieved in the BCS and BEC limits, respectively, is unchanged even for different tunneling-coupling ratios. In other words, the pair tunneling process inevitably occurs in

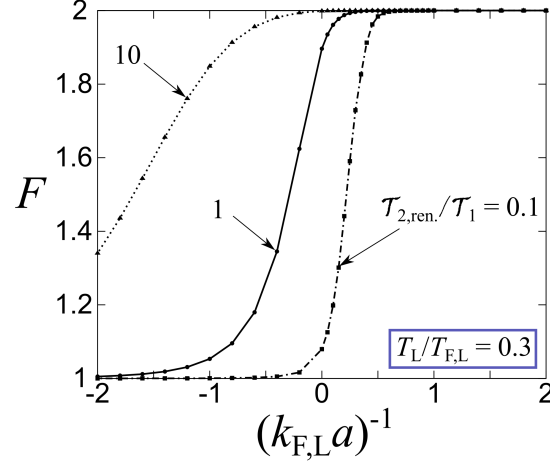


FIG. 6. Fano factor F throughout the BCS-BEC crossover at different tunneling-coupling ratio $\mathcal{T}_{2,\text{ren.}}/\mathcal{T}_1$. The temperature is taken as $T_L/T_{F,L} = 0.3$. One can see that F changes from 1 to 2 with increasing the interaction strength regardless of different $\mathcal{T}_{2,\text{ren.}}/\mathcal{T}_1$.

the strong-coupling regime even for an infinitesimally small pair-tunneling coupling \mathcal{T}_2 . This is a natural consequence in the sense that the system is dominated by bound molecules and hence there are no single-particle states in such a regime.

We note that the value of $\mathcal{T}_{2,\text{ren.}}/\mathcal{T}_1$ is associated with the potential barrier and the interaction strength [25]. While it is not so straightforward to estimate $\mathcal{T}_{2,\text{ren.}}/\mathcal{T}_1$ in each experimental setup, it is sufficient to observe F at the regime where the anomalously large tunneling current can be found [e.g., at unitarity observed in Ref. [7]] for our purpose of detecting the pair-tunneling current.